23rd ABCM International Congress of Mechanical Engineering
December 6-11, 2015, Rio de Janeiro, RJ, Brazil

LARGE EDDY SIMULATION AND AEROACOUSTICS OF SUPERSONIC JET FLOWS

Carlos Junqueira-Junior
Sami Yamouni
Instituto Tecnológico de Aeronáutica
junior.hmg@gmail.com
sami.yamouni@gmail.com

João Luiz F. Azevedo
Instituto de Aeronáutica e Espaço
joaoluiz.azevedo@gmail.com

William R. Wolf
Universidade Estadual de Campinas
wolf@fem.unicamp.br

Abstract. *Current design constraints have encouraged the studies of aeroacoustics fields around compressible jet flows. The present work addresses the numerical study of unsteady turbulent jet flows for aeroacoustic analyses of main engine rocket plumes. A novel large eddy simulation (LES) tool is developed in order to reproduce high fidelity results of compressible jet flows which could be used for aeroacoustic studies with the Ffowcs Williams and Hawkings approach. The numerical solver is an upgrade of an existing Reynolds-averaged Navier-Stokes solver previously developed in the group. The original framework is rewritten in a modern fashion and intensive parallel computation capabilities have been added to the code. The LES formulation is written using the finite difference approach. The energy equation is carefully discretized in order to model the energy equation of the filtered Navier-Stokes formulation. The classical Smagorinsky model is the chosen subgrid scale closure for the present work. Numerical simulations of perfectly expanded jets are performed and compared with the literature in order to validate the new solver. Flow results are used for an initial evaluation of the noise radiated from the rocket plume.*
Keywords: *LES, Jet Flows, Turbulence Modeling and Aeroacoustics*

1. INTRODUCTION

One of the main design issues related to launch vehicles lies on noise emission originated from the complex interaction between the high-temperature/high-velocity exhaustion gases and the atmospheric air. These emissions yield very high noise levels, which must be minimized due to several design constraints. For instance, the resulting pressure fluctuations can damage the solid structure of different parts of the launcher by vibrational acoustic stress. Therefore, it is a design constraint to consider the loads resulting from acoustic sources in the structural dimensioning of large launch vehicles during the take off and also during the transonic flight. Moreover, one cannot neglect the energy dissipation effect caused by the acoustic waves generated even if the vehicles is far from the ground. Theoretically, all chemical energy should be converted into kinectic energy. However, in reallity, the noise generation consumes part of the chemical energy.

The acoustic design constraints have encouraged the studies of aeroacoustic fields around compressible jet flows. Instituto de Aeronautica e Espaço (IAE) in Brazil is interested in this flow configuration for rocket design applications. Unsteady property fields of the flow are necessary for the aerocoustic studies. Therefore, the present work addresses the development of a new numerical tool for the study of unsteady turbulent compressible jet flows for aeroacoustic applications. The novel code uses the large eddy simulation (LES) formulation due to recent successful results of such approach for similar flow configurations (Bodony and Lele, 2005; Garnier *et al.*, 2009). Such formulation is able to reproduce high fidelity results for compressible jet flows, which, in turn, could be used for aeroacoustic studies using the Ffowcs Williams and Hawkings approach (Wolf *et al.*, 2012).

The solver is an upgrade of a finite difference Reynolds-averaged Navier-Stokes (RANS) solver developed to study turbulent flows for aerospace applications (Bigarella, 2002). Generally, LES calculations demand very dense grids. Hence, high performance computing (HPC) is a requirement for such simulations. Dynamic memory allocation and parallel computation capabilities have been added to the legacy code (Bigarella, 2002). The communication between processors is performed by message passing interface (MPI) protocols. The CFD general notation system (CGNS) is also included in the numerical tool. The LES formulation is written using the finite difference approach. Inviscid numerical fluxes are calculated using a second-order accurate centered scheme with the explicit addition of artificial dissipation. A five-step second-order accurate Runge-Kutta scheme is the chosen time marching method.

The System I formulation (Vreman, 1995) is used here in order to model the filtered terms of the energy equation. The Smagorinsky (1963) model is the chosen model to calculate the components of the subgrid scale (SGS) tensor. The Eidson (1985) hypothesis is the chosen model to calculate the subgrid scale terms of the filtered energy equation. For the sake of simplicity, only perfectly expanded jet configurations are studied in the current work. The LES tool is validated through a comparison of results of perfectly expanded jets with numerical (Bodony and Lele, 2005; Mendez *et al.*, 2010) and experimental (Tanna, 1977; Bridges and Wernet, 2008) data. Moreover, the computational performance of the solver is evaluated and discussed. Flow results are used for an initial evaluation of the noise radiated from the rocket plume.

2. LARGE EDDY SIMULATION FORMULATION

The numerical strategy used in the present study is based on the System I filtered compressible Navier-Stokes equations (Vreman, 1995) formulated as

$$\frac{\partial \overline{\rho}}{\partial t} + \frac{\partial}{\partial x_j}\left(\overline{\rho}\widetilde{u_j}\right) = 0\,, \tag{1}$$

$$\frac{\partial}{\partial t}\left(\overline{\rho}\widetilde{u_i}\right) + \frac{\partial}{\partial x_j}\left(\overline{\rho}\widetilde{u_i}\widetilde{u_j}\right) + \frac{\partial \overline{p}}{\partial x_i} - \frac{\partial \check{\tau}_{ij}}{\partial x_j} = -\frac{\partial}{\partial x_j}\left[\sigma_{ij} - \left(\overline{\tau_{ij}} - \check{\tau}_{ij}\right)\right]\,, \tag{2}$$

$$\frac{\partial \overline{\rho}\check{E}}{\partial t} + \frac{\partial\left(\overline{\rho}\check{E} + \overline{p}\right)\widetilde{u_j}}{\partial x_j} - \frac{\partial \check{\tau}_{ij}\widetilde{u_i}}{\partial x_j} + \frac{\partial \check{q}_j}{\partial x_j} = -B_1 - B_2 - B_3 + B_4 + B_5 + B_6 - B_7\,, \tag{3}$$

in which t and x_i are independent variables representing time and spatial coordinates of a Cartesian coordinate system $\mathbf{x}$, respectively. The components of the velocity vector $\mathbf{u}$ are written as u_i, and $i = 1, 2, 3$. Density, pressure and total energy per mass unit are denoted by ρ, p and E, respectively. $\overline{(\cdot)}$ stands for filtered properties and $\widetilde{(\cdot)}$ stands for Favre averaged properties. The filtered heat flux, $\check{q}_j$, is given by

$$\check{q}_j = \left[\kappa(\tilde{T})\right]\frac{\partial \tilde{T}}{\partial x_j}\,, \tag{4}$$

where $\tilde{T}$ is the averaged static temperature and κ is the thermal conductivity, which can by expressed by

$$\kappa(T) = \left[\mu(T)\right]\frac{C_p}{Pr}\,. \tag{5}$$

The thermal conductivity is a function of the specific heat at constant pressure, Cp, of the Prandtl number, Pr, which is equal to 0.72 for air, and of the dynamic viscosity, μ. The last is calculated using the Sutherland Law,

$$\mu(T) = \mu_\infty\left(\frac{T}{T_\infty}\right)^{\frac{3}{2}}\frac{T_0 + S_1}{T + S_1} \quad \text{with } S_1 = 110.4K\,. \tag{6}$$

In the present work, $\check{\tau}_{ij}$ is calculated using the Stokes hypothesis for Newtonian fluids,

$$\check{\tau}_{ij} = 2\left[\mu(\tilde{T})\right]\left(\check{S}_{ij} - \frac{1}{3}\delta_{ij}\check{S}_{kk}\right)\,, \tag{7}$$

in which $\check{S}_{ij}$, components of rate-of-strain tensor, is given by

$$\check{S}_{ij} = \frac{1}{2}\left(\frac{\partial \widetilde{u_i}}{\partial x_j} + \frac{\partial \widetilde{u_j}}{\partial x_i}\right)\,. \tag{8}$$

In order to close the system of equations the density, the static pressure and the static temperature are correlated by the equation of state given by

$$\overline{p} = \overline{\rho}R\tilde{T}\,, \tag{9}$$

where R is the gas constant, written as

$$R = C_p - C_v\,, \tag{10}$$

and C_v is the specif heat at constant volume. The System I formulation (Vreman, 1995) neglects the double correlation term of the total energy per mass unity and writes

$$\overline{\rho E} = \overline{\rho}\check{E} = \frac{\overline{p}}{\gamma - 1} + \frac{1}{2}\rho\tilde{u}_i\tilde{u}_i\,, \tag{11}$$

in which γ is the specif heat ratio written as $\gamma = Cp/Cv$. The components of the SGS stress tensor, σ, are given by

$$\sigma_{ij} = \overline{\rho}\left(\widetilde{u_i u_j} - \widetilde{u}_i \widetilde{u}_j\right) , \tag{12}$$

and the SGS B_i terms are written as

$$B_1 = \frac{1}{(\gamma - 1)} \frac{\partial}{\partial x_j}\left(\overline{p u_j} - \overline{p}\widetilde{u}_j\right) = \frac{\partial C_v \mathcal{Q}_j}{\partial x_j} , \tag{13}$$

$$B_2 = \overline{p\frac{\partial u_k}{\partial x_k}} - \overline{p}\frac{\partial \widetilde{u_k}}{\partial x_k} = \Pi_{dil} , \tag{14}$$

$$B_3 = \frac{\partial}{\partial x_j}\left(\sigma_{kj}\widetilde{u_k}\right) , \tag{15}$$

$$B_4 = \sigma_{kj}\frac{\partial}{\partial x_j}\widetilde{u_k} , \tag{16}$$

$$B_5 = \overline{\tau_{kj}\frac{\partial}{\partial x_j}u_k} - \overline{\tau_{ij}}\frac{\partial}{\partial x_j}\widetilde{u_k} = \mathcal{E} , \tag{17}$$

$$B_6 = \frac{\partial}{\partial x_j}\left(\overline{\tau_{ij}\widetilde{u}_i} - \check{\tau}_{ij}\widetilde{u}_i\right) = \frac{\partial \mathcal{D}}{\partial x_j} , \tag{18}$$

$$B_7 = \frac{\partial}{\partial x_j}\left(\overline{q_j} - \check{q}_j\right) , \tag{19}$$

where $\mathcal{Q}_j$ is the SGS temperature flux, written as

$$\mathcal{Q}_j = \overline{\rho}\left(\widetilde{u_j T} - \widetilde{u}_j\widetilde{T}\right) , \tag{20}$$

Π_{dil} is the SGS pressure-dilatation term, $\mathcal{E}$ is the SGS viscous dissipation and $\mathcal{D}$ is the SGS viscous diffusion term.

3. SUBGRID SCALE MODELING

The SGS terms presented in Eqs. (2) and (3) cannot be directly calculated. Subgrid scale models are necessary in order to close the LES set of equations. The closure models presented here are based on homogeneous turbulence theory, which is usually developed in spectral space as an atempt to quantify the interaction between the different scales of turbulence.

3.1 Subgrid Scale Viscosity

The SGS stress tensor is here calculated using the concept that the forward energy cascade is analogous to the molecular mechanisms represented by the molecular viscosity whose mathematical structure follows the Boussinesq (1877) hypothesis to explicitly introduce the subgrid scale viscosity, μ_{sgs},

$$\sigma_{ij}^{d} = \sigma_{ij} - \frac{1}{3}\delta_{ij}\sigma_{kk} = -2\mu_{sgs}\left(\check{S}_{ij} - \frac{1}{3}\check{S}_{kk}\right) . \tag{21}$$

The isotropic portion of the SGS stress tensor is generally weak with respect to the thermodynamic pressure (Erlebacher *et al.*, 1992). Therefore, σ_{kk} is neglected in the present paper and σ_{ij} is written as

$$\sigma_{ij} = -2\mu_{sgs}\left(\check{S}_{ij} - \frac{1}{3}\check{S}_{kk}\right) . \tag{22}$$

The Smagorinsky model (Smagorinsky, 1963; Lilly, 1965) is used to calculate the SGS viscosity and it is given by

$$\mu_{sgs} = \overline{\rho}\left(C_s\Delta\right)^2\left(2\check{S}_{ij}\check{S}_{ij}\right)^{\frac{1}{2}} , \tag{23}$$

and C_s is the Smagorinsky constant. Several attempts can be found in the literature regarding the evaluation of the Smagorinsky constant. The value of this constant is adjusted to improve the results of different flow configurations. In pratical terms, the Smagorinsky constant assumes value ranging from 0.1 to 0.2 depending on the flow. The present work uses $C_s = 0.18$ as suggested by Lilly (1967).

3.2 Subgrid Scale Modeling of the Energy Equation

Some of the SGS terms within the System I formulation (Vreman, 1995) are not directly computable. Therefore, modeling is applied in order to close the system. Several papers in the literature (Garnier *et al.*, 2009; Erlebacher *et al.*, 1992; Moin *et al.*, 1991; Martín *et al.*, 2000; Lenormand *et al.*, 2000; Coleman *et al.*, 1995) evaluate the relevance of the SGS terms on different applications. The LES community commonly uses the hypothesis of Eidson (1985), which assumes that the energy transfer from the resolved scales is proportional to the gradient of the resolved temperature (Garnier *et al.*, 2009). The proportionality coefficient is the subgrid scale conductivity, κ_{sgs}, which is linked to the subgrid scale viscosity through the relation

$$\kappa_{sgs} = \frac{\overline{\rho}\,\nu_{sgs}\,C_p}{Pr_{sgs}}\,, \tag{24}$$

in which Pr_{sgs} is the SGS Prandtl number. The eddy-damped quasi-normal Markovian (EDQNM) theory (Lesieur, 2008) considers $Pr_{sgs} = 0.6$. In the present work, the concept of SGS conductivity, κ_{sgs}, is used in order to model $B_1 + B_2$, *i.e.*,

$$B_1 + B_2 = -\frac{\partial}{\partial x_j}\left(\kappa_{sgs}\frac{\partial \tilde{T}}{\partial x_j}\right)\,, \tag{25}$$

Following the work of Larchêveque (2003), B_4, B_5, B_6 and B_7 are neglected in the present paper.

3.3 Shear-Stress Tensor Modeling

The difference between the shear-stress tensors at the right-hand side of the momentum equations is neglected in the present work,

$$\overline{\tau_{ij}} - \check{\tau}_{ij} = 0 \tag{26}$$

4. NUMERICAL FORMULATION

The governing equations previously described are discretized in a structured finite difference context for general curvilinear coordinate system (Bigarella, 2002). The numerical flux is calculated through a central difference scheme with the explicit addition of the anisotropic scalar artificial dissipation of Turkel and Vatsa (1994). The time integration is performed by an explicit, 2nd-order, 5-stage Runge-Kutta scheme (Jameson and Mavriplis, 1986; Jameson *et al.*, 1981). Conserved properties and artificial dissipation terms are properly treated near boundaries in order to assure the physical correctness of the numerical formulation.

The original solver was created for two flow configurations, the 3D zero-pressure gradient flat plate and the 3D axisymmetric flows. For the configuration of interest here, the types of boundary conditions include a combination of the boundary conditions coming from the two original cases: entrance and exit conditions, centerline and far fields conditions. Considering the new case as perfectly 3D, instead of the symmetric condition, a new periodic condition is implemented in the azimuthal direction. The reader can find a more detailed description of the numerical formulation and boundary condition in Junqueira-Junior *et al.* (2015).

5. NUMERICAL RESULTS

The present section is devoted to a preliminary study of a supersonic perfectly expanded jet flow. Results are compared with analytical, numerical and experimental data from the literature (Bodony and Lele, 2005; Mendez *et al.*, 2010; Tanna, 1977; Bridges and Wernet, 2008; Lo *et al.*, 2012; Laufer *et al.*, 1976). First LES results using the Smagorinsky (1963) SGS turbulence closure are discussed. The flow is characterized by an unheated perfectly expanded inlet jet with a Mach number of 1.4 at the domain entrance. Therefore, the pressure ratio, $PR = P_j/P_\infty$, and the temperature ratio, $TR = T_j/T_\infty$, between the jet exit and the ambient freestream are equal to one, $PR = 1$ and $TR = 1$. The time step used in the simulation is constant and equal to 2.5×10^{-5} in dimensionless form. The Reynolds number of the jet is $Re = 1.57 \times 10^6$. The radial and longitudinal dimensions of the smallest cell of the computational domain are given by $(\Delta \underline{r})_{min} = 0.002$ and $(\Delta \underline{x})_{min} = 0.0126$, respectively, again in dimensionless form. This cell is located in the shear layer of the jet, at the entrance of the computational domain. The number of points in the azimuthal direction is $N_\theta = 180$. The mesh domain is composed by 14.4 million points. The present mesh reproduces well the main geometric characteristics of the reference grid (Mendez *et al.*, 2010).

Generally, compressible jet flow studies performed in the literature present mean field properties. However, as the present simulation is not statistically converged yet, mean quantities could not be calculated. As an example, using the same flow configuration, Mendez *et al.* (2010) needed 300 characteristic times, $\mathcal{T}_\infty$, to obtain averages. Here, $\mathcal{T}_\infty$ is defined as the ratio between the diameter D and the ambient sound speed a_∞. The simulation time of the cited reference corresponds approximately to four flow through times. One flow through time is the time for a particle to cross the entire domain from the jet entrance to the domain exit. The reader should remember that, as $TR = 1$ and $a_j = a_\infty$, the characteristic time in the present work is equal to that reported in the work of Mendez *et al.* (2010). In the present work, the code assessment of the supersonic jet flow is made by observing the last obtained snapshot. This snapshot corresponds to 18.5 $\mathcal{T}_j$ which is far less than the computational time in the reference. However, the authors chose to start the analysis of the jet flow using this field. Figure 1(a) displays instantaneous fields of pressure and vorticity of the jet at that instant. The jet is entering into the domain at the left and evolves towards the right of the domain. As the flow has been initialized from stagnation conditions and not, for instance, from a converged RANS solution, a front pressure shock wave is preceding the first vortical structures. Figure 1(b) focuses on the jet flow entrance. At the beginning of the mixing layer, thin axisymmetrical vortices are growing and pairing, leading then to turbulent transition at approximatively $x = 1.5D$. This figure also displays Mach waves emitted by the mixing layer, displaying a downstream directivity, retrieving traditional trends (Bodony and Lele, 2005; Mendez *et al.*, 2010; Tanna, 1977; Bridges and Wernet, 2008; Lo *et al.*, 2012; Laufer *et al.*, 1976). One can notice that the strongest acoustic sources match the coherent structure locations, identifiable by the condensed vorticity rings.

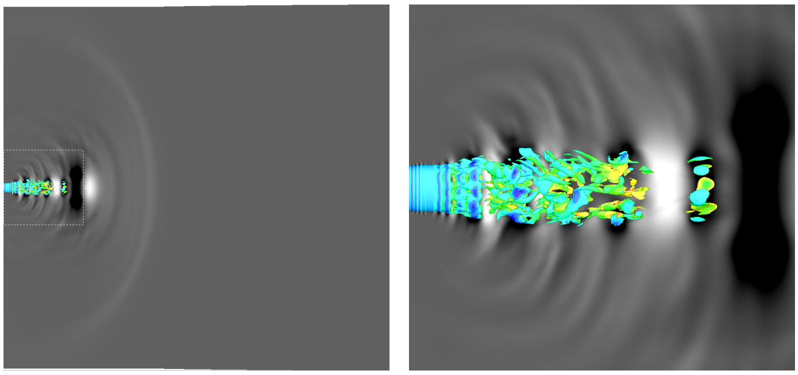

(a) (b)

Figure 1. Instantaneous pressure and vorticity fields for the perfectly expanded supersonic jet. The gray scale contours show $\underline{p}$ from 0.4 to 0.9, while a dimensionless iso-contour of vorticity of magnitude $|\omega| D/U_j = 10$ is colored by the streamwise velocity $\underline{u}$ from -0.2 (blue) to 1.4 (red).

Figure 2(a) presents the radial profile of the streamwise velocity component at $x = 2.5D$ and compares it with the averaged numerical and experimental profiles from Mendez *et al.* (2010) and Bridges and Wernet (2008), respectively. The centerline values of the velocity profile are overestimated in the current simulation when compared to the references. This difference is expected since a flat inlet boundary profile is used for this simulation while a laminar profile, necessarily thicker, is used in the numerical reference work. However, keeping in mind that the current profile is instantaneous, a fair agreement is obtained. Similar observations can be made on the results comparing the centerline streamwise velocity components, shown in Figure 2(b). The values in the potential core, corresponding to the jet area until $U = 0.95 \cdot U_j$, compare well with the references. Moreover, one can expect that, as the jet will grow downstream, the decreasing slope after the potential core will raise to meet the reference curves, confirming thus the good trend of the present simulation.

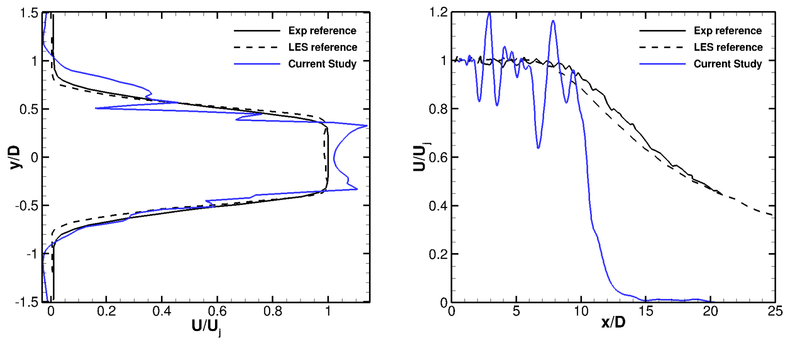

(a) (b)

Figure 2. Comparison between numerical and experimental streamwise velocity component profiles along the centerline (a), and radial profiles at $x = 2.5D$. Instantaneous results from the present study are compared with LES results (Mendez *et al.*, 2010) and experimental ones (Bridges and Wernet, 2008).

Another visualization of this jet flow is shown in Fig. 3. It is possible to observe the evolution of the vorticity looking at different cross-flow planes from $\underline{x} = 0.1$ to 7.5. At the moment of this snapshot, slices located after the last streamwise position shown are irrelevant as the jet is not fully developed yet. From $\underline{x} = 0.1$ to 0.25, the mixing layer is getting thicker and it is axisymmetric as already observed in Fig. 1. Further downstream, the flow becomes completely three dimensional and is no longer axisymmetric, transitioning towards a turbulent state. Still, the turbulent vortical structures are larger than already observed in the literature (Mendez *et al.*, 2010; Bres *et al.*, 2012). This is due to the low order of the computational code and the barely acceptable refinement of the grid for LES simulations. The mixing layer continues widening as one moves downstream. One can clearly expect that the mixing layer will spread until the jet centerline near the end of the potential core.

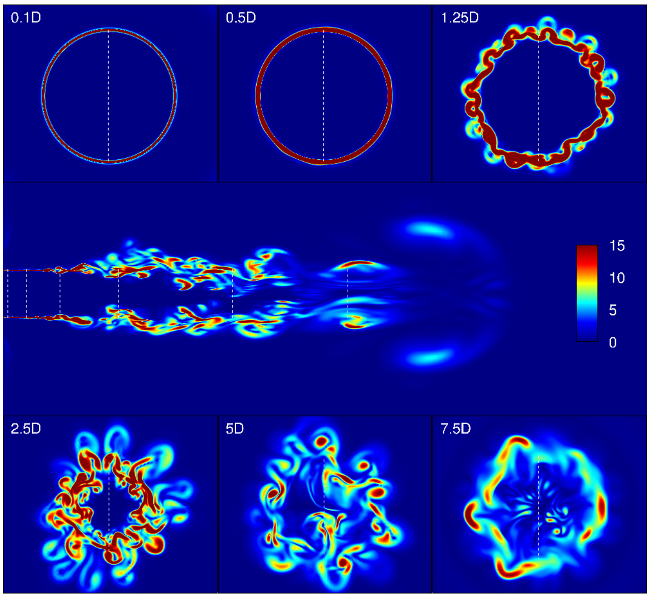

Figure 3. Instantaneous vorticity magnitude for the present simulation at $M = 1.4$.

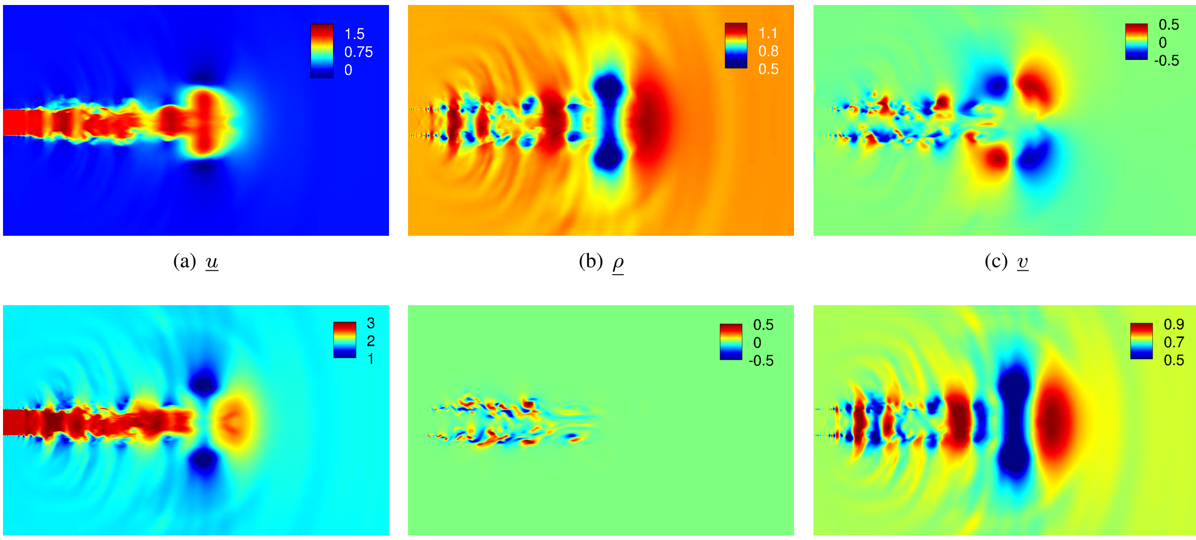

(a) $\underline{u}$ (b) $\underline{\rho}$ (c) $\underline{v}$

(d) $\underline{E}$ (e) $\underline{w}$ (f) $\underline{p}$

Figure 4. Instantaneous properties of the perfectly expanded supersonic jet flow.

Finally, flow properties are displayed in Fig. 4. In this two dimensional snapshot, radial and azimuthal velocity components correspond to vertical and spanwise velocity components, respectively. The $\underline{v}$ and $\underline{w}$ velocity components are of the same order of magnitude in the jet mixing layer turbulent region, illustrating thus the three dimensional turbulent behaviour of the jet mixing layer. Looking at the second column of Figure 4, one can observe weak shock cells in the instantaneous density, total energy and pressure fields. Downstream directivity patterns are very similar to those seen in the reference work (Mendez *et al.*, 2010; Bres *et al.*, 2012), confirming one more time that the current simulation is evolving towards the correct trends.

6. CONCLUDING REMARKS

The current work is based on the development of novel large eddy simulation tool for the study of supersonic jet flows. The numerical code background is a RANS solver designed for rocket flow configurations. The original solver is improved in order to simulate supersonic jet flows using an LES formulation within a multiprocessor environment.

Large eddy simulations of a perfectly expanded supersonic jet flow configuration are performed. The classical Smagorinsky model is used to calculate the subgrid terms. Results obtained in this work do not allow the calculation of statistically time-averaged properties since the simulation only ran during a very limited time period. However, since the aim of the paper is mostly to validate the LES computational tool, the authors believe that the results here included should provide enough information to allow evaluation of the trends of jet physics. Early quantitative comparisons with numerical (Mendez *et al.*, 2010) and experimental (Bridges and Wernet, 2008) reference work are obtained. The jet mixing layer is showing strong instabilities evolving towards a turbulent state. The classical downstream directivity pattern already observed in the literature (Bodony and Lele, 2005; Mendez *et al.*, 2010; Tanna, 1977; Bridges and Wernet, 2008; Laufer *et al.*, 1976) is retrieved. The velocity profiles also show a good agreement with the references.

Finally, regarding the low order, more dissipative numerical scheme, the early results show a fairly good agreement with the references, indicating that grid refinement could probably resolve such issues. Hence, for future simulations, a much more refined new grid should be used to counterbalance the dissipation induced by the numerical scheme. In addition, the computational code needs to be further improved through the availability of more sophisticated time-marching schemes. For instance, the time step used in the present simulations is one hundred times smaller than the one used in literature (Mendez *et al.*, 2010), leading to a prohibitive simulation cost. Hence, a new time integration method should be implemented, such as a preconditioned dual-time step procedure (Pandya *et al.*, 2003). Furthermore, acoustic predictions of the far field noise using the Ffowcs Williams and Hawkings analogy will be performed using the reference work of Wolf and Lele (2011). Results will be compared one more time with the numerical studies of Mendez *et al.* (2010), Bres *et al.* (2012) and Khalighi *et al.* (2010). The influence of the inlet boundary profile on the acoustics will also be investigated.

7. ACKNOWLEDGEMENTS

The authors gratefully acknowledge the partial support for this research provided by Conselho Nacional de Desenvolvimento Científico e Tecnológico, CNPq, under the Research Grants No. 309985/2013-7, No. 400844/2014-1, No. 443839/2014-0 and No. 574004/2008-4. This work is also supported by Fundação Coordenação de Aperfeiçoamento de Pessoal de Nível Superior, CAPES, through a Ph.D. scholarship for the first author. The authors are also indebted to the partial financial support received from Fundação de Amparo à Pesquisa do Estado de São Paulo, FAPESP, under the Research Grants No. 2008/57866-1, No. 2013/07375-0 and No. 2013/21535-0. This work has been conducted with the computational resources of the National Supercomputing Center (CESUP), from Universidade Federal do Rio Grande do Sul, UFRGS, in Brazil, besides those available from the FAPESP CEPID–CeMEAI project previously cited.

8. REFERENCES

Bigarella, E.D.V., 2002. *Three-Dimensional Turbulent Flow Over Aerospace Configurations*. M.Sc. Thesis, Instituto Tecnológico de Aeronáutica, São José dos Campos, SP, Brasil.

Bodony, D. and Lele, S.K., 2005. "On using large-eddy simulation for the prediction of noise from cold and heated turbulent jets". *Physics of Fluids*, Vol. 17, No. 8. doi:10.1063/1.2001689.

Boussinesq, M.J., 1877. "Essai sur la théorie des eaux courantes". In *In: Mémoires Présentés par Divers Savants à l'Academie des Sciences, tome XXIII*, Imprimerie Nationale, pp. 43–47.

Bres, G.A., Nichols, J.W., Lele, S.K. and Ham, F.E., 2012. "Towards best practices for jet noise predictions with unstructured large eddy simulations". In AIAA Paper No. 2012-2965*, Proceedings of the 42nd AIAA Fluid Dynamics Conference and Exhibit*. New Orleans, Louisiana.

Bridges, J. and Wernet, M.P., 2008. "Turbulence associated with broadband shock noise in hot jets". *AIAA paper*, Vol. 2834, p. 2008.

Coleman, G.N., Kim, J. and Moser, R.D., 1995. "A numerical study of turbulent supersonic isothermal-wall channel flow". *Journal of Fluid Mechanics*, Vol. 305, pp. 159–183. doi:10.1017/S0022112095004587.

Eidson, T.M., 1985. "Numerical simulation of the turbulent rayleigh–bénard problem using subgrid modelling". *Journal of Fluid Mechanics*, Vol. 158, pp. 245–268. doi:10.1017/S0022112085002634.

Erlebacher, G., Hussaini, M.Y., Speziale, C.G. and Zang, T.A., 1992. "Toward the large-eddy simulation of compressible turbulent flows". *Journal of Fluid Mechanics*, Vol. 238, pp. 155–185. doi:10.1017/S0022112092001678.

Garnier, E., Adams, N. and Sagaut, P., 2009. *Large Eddy Simulation for Compressible Flows*. Springer. doi:10.1007/978-90-481-2819-8.

Jameson, A. and Mavriplis, D., 1986. "Finite volume solution of the two-dimensional euler equations on a regular triangular mesh". *AIAA Journal*, Vol. 24, No. 4, pp. 611–618.

Jameson, A., Schmidt, W. and Turkel, E., 1981. "Numerical solutions of the euler equations by finite volume methods using runge-kutta time-stepping schemes". In AIAA Paper 81–1259*, Proceedings of the AIAA 14th Fluid and Plasma Dynamic Conference*. Palo Alto, Californa, USA.

Junqueira-Junior, C., Yamouni, S., Azevedo, J.L.F. and Wolf, W.R., 2015. "Large Eddy Simulations of Supersonic Jet Flows for Aeroacoustic Applications". In *To Appear in the 33rd Applied Aerodynamics Conference – AIAA*. Jun., Dallas,Texas, USA.

Khalighi, Y., Ham, F., Moin, P., Lele, S.K., Colonius, T., Schlinker, R.H., Reba, R.A. and Simonich, J., 2010. "Unstructured large eddy simulation technology for prediction and control of jet noise". In *ASME Turbo Expo 2010: Power for Land, Sea, and Air*. American Society of Mechanical Engineers, pp. 57–70.

Larchêveque, M.L., 2003. *Simulation des Grandes Échelles de l'Écoulement Au-Dessus d'une Cavité*. Ph.D. thesis, Université Paris VI - Pierre et Marie Curie, Paris, France.

Laufer, J., Schlinker, R. and Kaplan, R., 1976. "Experiments on supersonic jet noise". *AIAA Journal*, Vol. 14, No. 4, pp. 489–497.

Lenormand, E., Sagaut, P., Phuoc, L.T. and Comte, P., 2000. "Subgrid-scale models for large-eddy simulations of compressible wall bounded flows". *AIAA Journal*, Vol. 38, No. 8, pp. 1340–1350. doi:10.2514/2.1133.

Lesieur, M., 2008. *Turbulence in Fluids*. Springer, Saint Martin d´Hères, France, 4th edition.

Lilly, D.K., 1967. "The representation of small-scale turbulence in numerical simulation experiments". In IBM Form No. 320-1951*, Proceedings of the IBM Scientific Computing Symposium on Environmental Sciences*. Yorktown Heights, N.Y., pp. 195–210.

Lilly, D.K., 1965. "On the computational stability of numerical solutions of time- dependent non-linear geophysical fluid dynamics problems". *Monthly Weather Review*, Vol. 93, No. 1, pp. 11–25. doi:10.1175/1520-0493(1965)093<0011:OTCSON>2.3.CO;2.

Lo, S.C., Aikens, K.M., Blaisdell, G.A. and Lyrintzis, A.S., 2012. "Numerical investigation of 3-d supersonic jet flows using large-eddy simulation". *International Journal of Aeroacoustics*, Vol. 11, No. 7, pp. 783–812.

Martín, M.P., Piomelli, U. and Candler, G.V., 2000. "Subgrid-scale models for compressible large-eddy simulations". *Theoretical and Computational Fluid Dynamics*, Vol. 13, No. 5, pp. 361–376. doi:10.1007/PL00020896.

Mendez, S., Shoeybi, M., Sharma, A., Ham, F.E., Lele, S.K. and Moin, P., 2010. "Large-eddy simulations of perfectly-expanded supersonic jets: Quality assessment and validation". In AIAA Paper No. 2010–0271. doi:10.2514/6.2010-271.

Moin, P., Squires, K., Cabot, W. and Lee, S., 1991. "A dynamic subgrid-scale model for compressible turbulence and scalar transport". *Physics of Fluids A: Fluid Dynamics (1989-1993)*, Vol. 3, No. 11, pp. 2746–2757. doi:10.1063/1.858164.

Pandya, S.A., Venkateswaran, S. and Pulliam, T.H., 2003. "Implementation of preconditioned dual-time procedures in OVERFLOW". In AIAA Paper No. 2003-0072*, Proceedings of the 41st AIAA Aerospace Sciences Meeting & Exhibit*. Reno, NV.

Smagorinsky, J., 1963. "General circulation experiments with the primitive equations: I. the basic experiment". *Monthly Weather Review*, Vol. 91, No. 3, pp. 99–164. doi:10.1175/1520-0493(1963)091<0099:GCEWTP>2.3.CO;2.

Tanna, H.K., 1977. "An experimental study of jet noise part I: Turbulent mixing noise". *Journal of Sound and Vibration*, Vol. 50, No. 3, pp. 405–428.

Turkel, E. and Vatsa, V.N., 1994. "Effect of Artificial Viscosity on Three-Dimensional Flow Solutions". *AIAA Journal*, Vol. 32, No. 1, pp. 39–45. URL http://doi.aiaa.org/10.2514/3.11948.

Vreman, A.W., 1995. *Direct and Large-Eddy Simulation of the Comperssible Turbulent Mixing Layer*. Ph.D. thesis, Universiteit Twente.

Wolf, W.R., Azevedo, J.L.F. and Lele, S.K., 2012. "Convective effects and the role of quadrupole sources for aerofoil aeroacoustics". *Journal of Fluid Mechanics*, Vol. 708, pp. 502–538.

Wolf, W.R. and Lele, S.K., 2011. "Aeroacoustic integrals accelerated by fast multipole method". *AIAA Journal*, Vol. 49, No. 7, pp. 1466–1477. doi:10.2514/1.J050861.

9. RESPONSIBILITY NOTICE

The authors are the only responsible for the printed material included in this paper.